



## EFFECTS OF DURATION OF SUBMARINE LANDSLIDES ON TSUNAMIS DUE TO THE 1771 YAEYAMA EARTHQUAKE

T. Ohsumi <sup>(1)</sup>, H. Fujiwara <sup>(2)</sup>, H. Hazarika <sup>(3)</sup>

<sup>(1)</sup> Principal Research Fellow, National Research Institute for Earth Science and Disaster Resilience (NIED); [t\\_ohsumi@bosai.go.jp](mailto:t_ohsumi@bosai.go.jp)

<sup>(2)</sup> Director, National Research Institute for Earth Science and Disaster Resilience (NIED); [fujiwara@bosai.go.jp](mailto:fujiwara@bosai.go.jp)

<sup>(3)</sup> Professor, Kyushu University, [hazarika@civil.kyushu-u.ac.jp](mailto:hazarika@civil.kyushu-u.ac.jp)

...

### **Abstract**

The Japanese Ministry of Education, Culture, Sports, Science, and Technology initiated the “Project for the Comprehensive Analysis and Evaluation of Offshore Fault Information” (The Project) in 2013. The objective of The Project is to contribute to assessment of earthquake and tsunami hazard in Japan’s seas by collecting off-shore fault information. The Project collects and consolidates reflection seismic data using the latest data processing technology where offshore fault information is missing. The data are collected from various institutions that have conducted fault evaluation surveys in the seas around Japan. The project reanalyzed the data and evaluated the faults using a consistent approach. NIED has reanalyzed the data of underground structures that were acquired by multiple institutions for the Japan Agency for Marine-Earth Science and Technology (JAMSTEC) and it has analyzed offshore fault information in the area of the southern Nansei Islands. In assuming the tsunami caused by the 1771 Yaeyama/Maiwa earthquake was associated with a submarine landslide, the present study reconstructed the shape of the shelf area around Yaeyama Islands and calculated the seabed deformation before the submarine landslide occurred.

In this study, we establish a method for reproducing tsunamis caused by submarine landslides. The simple technique applied by the plasticity of an experiment and the numerical analysis model, and the predictive method by the exercise dynamic submarine landslides model (kinematic model), has been used, with application for permission, for the nuclear power plant establishment. However, there are many uncertain factors. Furthermore, using a calculated slope failure duration, a verification was conducted for the 1771 Meiwa/Yaeyama tsunami. The maximum tsunami heights in the coastal area were calculated by applying the change directly in tsunami propagation analysis. The duration of the collapse of the assumed submarine landslide, about which little is known, was calculated using the Newmark sliding block method. A map of the geological structure of the seabed revealed that older Paleozoic age rocks are exposed from the Paleogene rocks on the slope. This study analyzed the propagation of tsunamis caused by landslides using the duration of the landslides and this study found that the influence of duration has considerable effect on maximum coastal tsunami height. The amount of seabed topographic variation did not follow the formula of Okada (1992); instead, it was entered directly and comparison was undertaken between the historical tsunami traces and the maximum coastal tsunami heights of each case. Thus, the tendency of the 1771 Yaeyama/Meiwa earthquake tsunami was reproduced. In addition, using the difference of landslide duration, this study performed analyses of tsunami propagation caused by landslides and this study found that the influence of duration has considerable effect on maximum coastal tsunami height. As a result, the reproducibility of the trace ( $K = 1.1$ , the value obtained by dividing the trace value by the calculated value) was good, confirming that the approach was effective.

*Keywords: Yaeyama/Maiwa earthquake; submarine landslides; Newmark sliding block method; tsunami*



## 1. Introduction

Offshore faults exist in the sea areas surrounding Japan. However, tsunamis due to submarine landslides are generally considered much bigger than caused by offshore fault deformation. It is believed that the tsunami associated with the 1771 Yaeyama/Meiwa earthquake was caused by a submarine landslide. This tsunami caused devastating damage and over 10,000 fatalities in the Miyako Islands archipelago.

In 2018, a strong earthquake with a moment magnitude of 7.5 occurred on the island of Sulawesi, Indonesia. This earthquake caused extensive liquefaction and, subsequently, submarine landslides characterized as liquefaction-induced flows caused tsunamis. The features of this earthquake have been referenced in explaining historical tsunami records.

For example, Imamura *et al.* (2001) [1] used information from this event to explain the historical tsunami records of the 1771 Yaeyama/Meiwa earthquake that devastated large areas of the Miyako and Yaeyama islands in the southwestern part of the Ryukyu Arc. It was assumed that this event was caused by an earthquake with a maximum class magnitude of  $M_w$  8.8. Conversely, based on detailed bathymetric and reflection seismic data, Okamura *et al.* (2018) [2] proposed a model for the source of the tsunami as a large-scale collapse on the accretionary prism along the trench, whereby a submarine landslide on the prism caused the aseismic tsunami. Using the circular slip method, Hiraishi *et al.* (2001) [3] also attributed the source of the tsunami to submarine landslides through numerical calculations based on an assumed duration for slope failure of 30–90 s.

This study investigated the effect of seabed structure on the generation of tsunamis triggered by submarine landslides through investigation of the shape of the island shelf in the Yaeyama area. By applying changes directly in the tsunami propagation analysis, we calculated the maximum tsunami heights in the coastal area. The duration of the collapse of the assumed submarine landslide, about which little is known, was calculated using the Newmark sliding block method.

The hazard presented by storm surges and flooding associated with global warming is increasing at a rapid rate. Therefore, it is highly important that regional studies contribute to disaster mitigation by securing safe urban function, while enhancing awareness of disaster prevention without causing concern for local residents. Internationally, it is important for Japan to demonstrate its contribution to disaster prevention as a nation facing many serious hazards.

## 2. Aseismic tsunamis

In relation to the 1771 Yaeyama/Meiwa earthquake, evidence of a submarine landslide has been confirmed through precise topographic investigation by Matsumoto and Kimura (1993) [4], who found it impossible to explain the height of tsunami traces based only on earthquake-scale fault displacement. Moreover, Hiraishi *et al.* (2001) [3] used the circular slip method to attribute the tsunami, associated with the 1771 Yaeyama/Meiwa earthquake, to mass movements generated by earthquake-induced landslides. In this study, we introduced a submarine landslide model using the circular slip method applied to the calculation of slope stability.

### 2.1 Water level fluctuation associated with volcanic activity

Active volcanic eruptions can cause aseismic tsunamis, as can the collapse of a volcanic edifice triggered by an earthquake. The Sakurajima eruption is an example of an undersea volcano near Japan known to have caused a tsunami (Toshiji and Ueda, 1996) [5]. Similarly, the 1883 eruption of Krakatoa in Indonesia was another such event (Normanbhoy N. and K. Satake, 1995 [6], Lander, J. F. and P. A. Lockridge, 1989 [7]). The onshore volcanic eruption of Komagatake (1640) in Hokkaido is an example where a tsunami was triggered by a landslide caused by the eruption (Yoshimoto *et al.*, 2008) [8], as also occurred following the Oshima-Oshima event in 1741 (Satake, 2007) [9], and the Matsubara Peninsula Mayuyama collapse in 1791–1792 (Tsuji and Hino, 1993) [10].



## 2.2 Water level fluctuation caused by mass movements such as landslides

Mass movements attributable to earthquakes can trigger landslides that produce tsunamis. In Japan, the Surugawan earthquake in 2009 was one such event (Baba, *et al.*, 2012) [11], as was the 1958 Lituya Bay earthquake in Alaska (USA) (Friz, *et al.*, 2009 [12], Weiss, *et al.*, 2009 [13]).

## 2.3 Water level fluctuation due to falling meteorites

Although it is unknown whether the occurrence of a tsunami in Japan has ever been caused by meteorite impact, it is thought that the extinction of the dinosaurs at the Cretaceous–Tertiary boundary was related to meteorite impact [14].

## 3. Equations Classification of submarine landslides

Ohyagi (2004) [15] cited Heezen and Ewing (1952) [16] who introduced the idea of a submarine landslide based on a study of the sea floor following the Grand Banks earthquake in southern Newfoundland ( $M_s$  7.2) in 1929, during which an undersea cable was broken by a submarine landslide. Macroscopically, a submarine landslide can be classified into one of five types of flow: a sediment gravity flow, turbidity current (turbulence), fluidized sediment flow, grain flow, or debris flow. Gibo *et al.* (2003) [17] classified the collapse form of Shimajiri-mudstone rock slopes as follows: strongly weathered fractured mudstone, crushed mudstone, normal consolidated mudstone, and mudstone containing a weak plane. This classification was directed to inland slopes and weathering of the seabed slope was not considered. Excluding the strongly weathered fractured mudstone and crushed mudstone, failure of the sedimentary rock can be assumed to have the strength degradation of normal consolidated mudstone. Thus, assuming that surface rupture contributed to the failures, this study assumed weak plane strength, we assumed the surface of rupture weak-plane strength, and set the surface of rupture.

## 4. Tsunami boulders within and around historical tsunami trace points

Representative points of historical tsunami traces, which were arranged by Hatori (1988) [18] based on Kato (1987) [19] and Kawana *et al.* (1987) [21] and so on as shown, were compared with calculated values for Ishigaki Island (ten points) and Miyako Island (three points).

Kawana *et al.* (1994) [20] were dated much older than the age of the 1771 Yaeyama/Meiwa Tsunami about 200 yr. BP. The boulders suggest that the Yaeyama Islands had been affected by devastating tsunamis around 600, 1,100, 2,000 and 2,400 yr. BP during the last 3,000 years with intervals of several hundred to one thousand years in the study area.

### 4.1 Ishigaki Island

#### 1) Tsunami Ufuishi (Ohama Elementary School): Fig.1



Park at Ohhama, which is said has a maximum diameter of height of  $\sim 6$  m. It is Skishima Great Tsunami result of the corals adhering to Ufuishi" is of 10.0 m and it is  $\sim 150$  m distance.

Fig. 1 "Tsunami Ufuishi" at the Sakihara Park of Ohhama



Other historical tsunami trace points and current picture shows **Fig.2**. Okinawa limestones are scattered, but it is unknown whether these are washed away by the tsunamis or the storm waves. However, it seems that the events that were shown by the tsunami are repeated. Goto *et al.* (2010) [21] classified the tsunamis or the storm waves. Storm wave boulders are distributed on the flat reef within 300 m landward of the reef edge in the Ryukyu Islands. However, tsunami boulders on the Ryukyu Islands are deposited far landward of this limit.

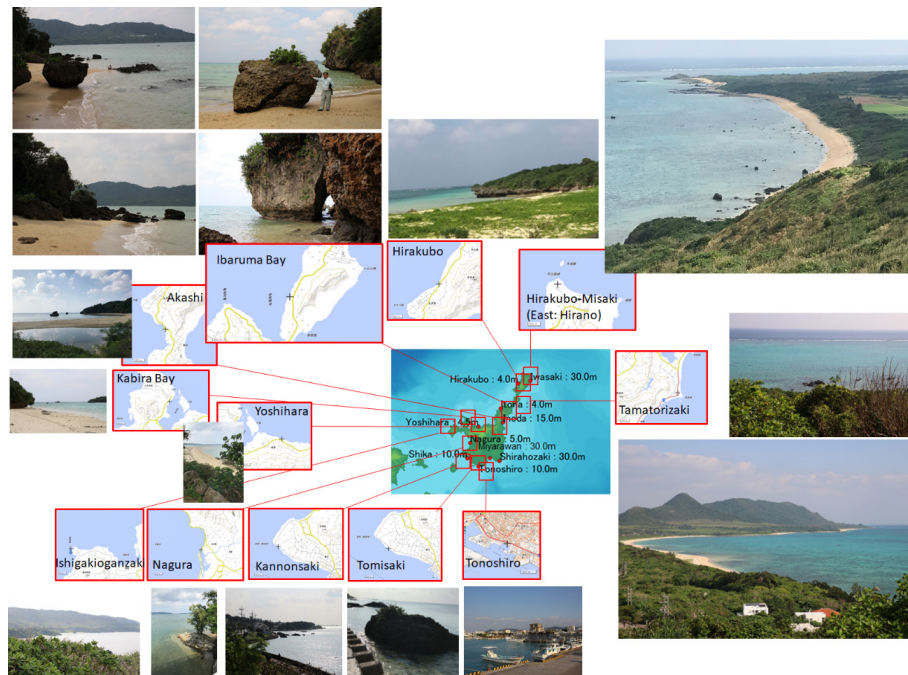


**Fig.2** Other historical tsunami trace points and current pictures (photo taken by T. Ohsumi on January 22-24, 2019)

## 2) Villages moved to uphill area: **Fig.3**

Shiraho Village is located in the southeastern part of Ishigaki Island. The population of Shiraho Village was 1,574, but in the 1771 Yaeyama/Meiwa tsunami, 1,546 were drowned, and the village was totally collapsed. The new village was rebuilt in the Uenoji of the northern plateau about 1 km northwest of the current village. However, this site was inconvenient and eventually returned to around 1793 where the previous village.

Miyara Village is located in Miyara Bay, southeast of Ishigaki Island. The village was under the cliff on the left bank of the Miyara River estuary. The population of Miyara Village was 1,221, but in the 1771 Yaeyama/Meiwa tsunami, 1,050 were drowned, and the village was totally collapsed. The village was built in Kanda, ~2 km northwest of the old village on the left bank of the Miyara River, and then relocated to the present location.

Ohama Village is a southern area of Ishigaki Island, and Ohhama village is the political and economic center of old Ohhama village along the present Route 390. The population of Ohama Village was 1,402, but in the 1771 Yaeyama/Meiwa tsunami, 1,287 were drowned, and the village was totally collapsed. The village has returned from uphill to previous location.

The population of Hirae Village was 1,178, but 560 people were drowned by the 1771 Yaeyama/Meiwa tsunami. The south side of the line from the east to the west of the village was collapsed, but 618 survived. The population of Maezato Village was 1,173, but in the 1771 Yaeyama/Meiwa tsunami, 908 were drowned.



313 people from Iriomote Village was relocated to the new village, and the total number of people left was 558, the original village was built in the area called Kajyauchibaru, north-northeast ~ 1.5km from Maezato Village.

The population of Ohkawa Village was 1,304 in 1760, but in the 1771 Yaeyama/Meiwa tsunami, 412 were drowned. 174 housing was swept away but there were no damage to the fame fields. In order to avoid tsunami damage, the village started relocating to Bunni in uphill 3 km north, but returned to its previous location in 1775 due to inconvenience.

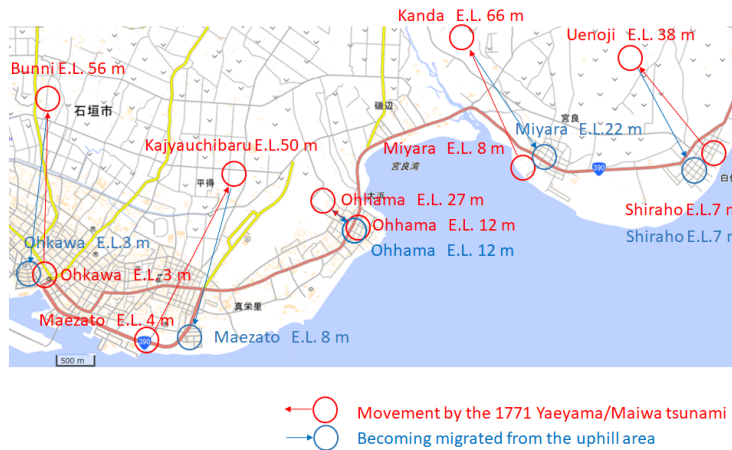


Fig.3 Villages moved to uphill area. [34, 35]

## 4.2 Miyako Island

### 1) Shimoji Island Monolith (Obi-Iwa): Fig. 4

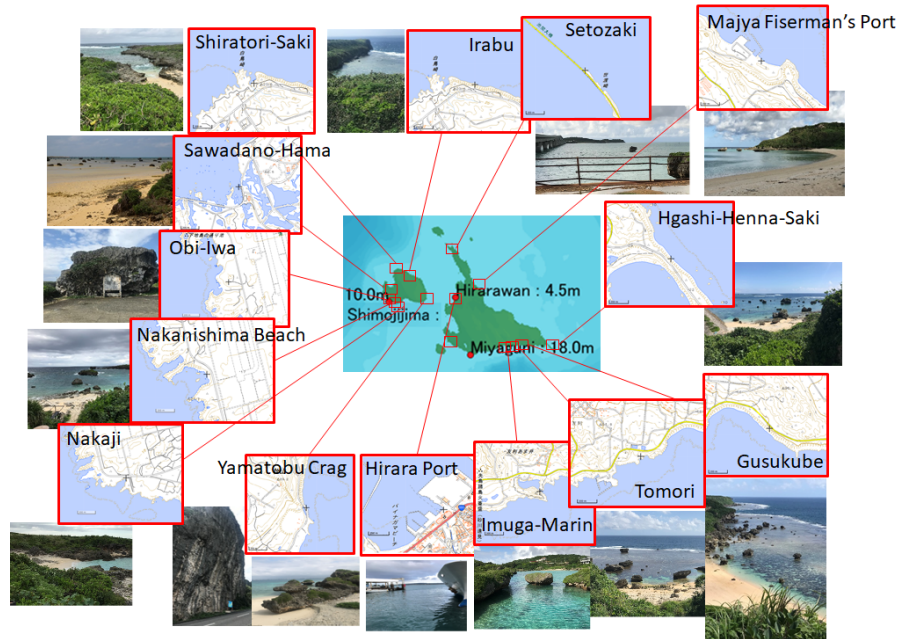
Shimoji Island Monolith is history tsunami trace points, tsunami run-up was 10 m. This boulder is 12.5 m high. This ground level is 12 m (data source from DEM10B). There is a notch at the height of ~10 m, this boulder was the position of the former seawater level. Other history tsunami trace points and current picture shows Fig. 4-26.



Fig. 4 Shimojijima Monolith (Obi-Iwa), a: Front view of the Shimojijima Monolith

### 2) Villages moved to uphill area

According to the ancient document "Kyuyou" [22], Miyakoku, Shinri, Sunagawa, Yoshimoto Motohima in the Motohima area was considered a village site destroyed by the Yaeyama/Meiwa tsunami. Fig. 5 shows the bird view of the survey area of the Motojima Ruins. Amai Well (24.73 N, 125.35 E; Elevation 16 m, Fig. 6) was for Tomori, Uruka and Shinzato residents, before the water supply has spread in Gusukube in 1965, this well begins drinking water. This well was used a precious water resource for a long time even after moving to the current colony, before the 1771 Yaeyama/Meyama tsunami.



**Fig. 5** Other history tsunami trace points and current pictures  
(photo taken by T. Ohsumi on February 20-22, 2019)

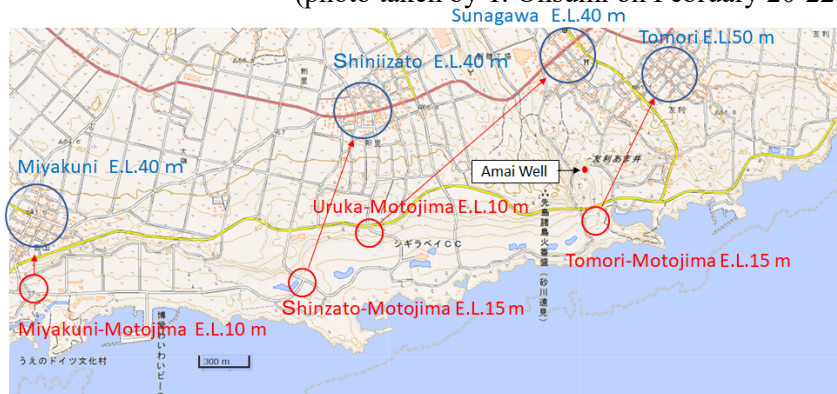


**Fig. 6** Motojima villages moved to uphill area.

## 5. Seabed topographic data

### 5.1 Island shelf points

As part of the “Project for the Comprehensive Analysis and Evaluation of Offshore Fault Information” (The Project), initiated in 2013 by the Japanese Ministry of Education, Culture, Sports, Science, and Technology, this study used the Red Relief Image Map (RRIM) method to visualize the seabed topography of the area around the southern Nansei Islands [23]. The RRIM method is based on multilayered topographic information computed from gridded three-dimensional digital elevation model data. An RRIM can be used to visualize the topographic slope, concavities, and convexities without requirement for any special geomatics or mapping information. From the topographic data of the seabed in the generated RRIM, it was possible to identify submarine landslide points in the Yaeyama area, the insular slopes of the forearc basin, sliding earth masses deposited by landslides, and points where seabed alluvial fans had formed. The lip-surface conduits in the direction of the insular slopes near Yaeyama Islands are shown in **Fig. 7**.

The solid white line in the figure shows the submarine landslide occurrence in region A, where the spread of the seafloor alluvial fan is observed, and the yellow broken line shows the submarine landslide occurrence in region B, which also appears continuous.

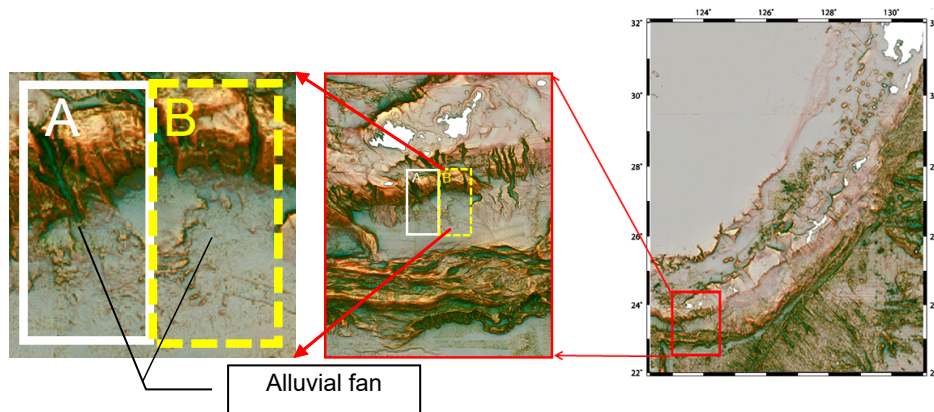


**Fig. 7** Seabed topography of the area around the Nansei Islands produced by the Red Relief Image Map visualization method: Solid white line shown in the figure, the submarine landslide occurrence A region. Yellow broken line shows the submarine landslide occurrence B region. (Courtesy of JAMSTEC)

### 5.2 Analysis section

The seabed topographic data and slide points in the RRIM represent the current situation, *i.e.*, after the occurrence of landslides. As stability analyses are performed on seabed topographic data before the occurrence of a landslide, we had to infer the seabed topographic data before the occurrence of a landslide in this study. A cross section of the current seabed topography is shown in **Fig. 8**. Ohyagi (2004) [15] considered the submarine landslide a turbidity current, but considering the simplification of the method, it is set with a circular slip shape, and the slope failure volume and sedimentation volume are set to be equivalent.

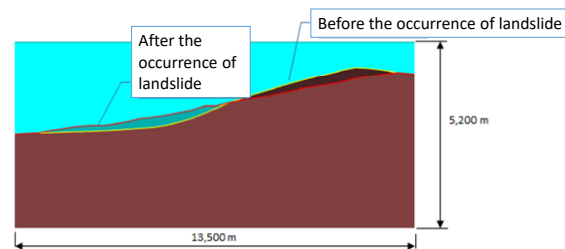


**Fig. 8** Topographic cross section of the current seabed

### 5.3 Submarine landslide points

Okamura *et al.* (2018) [2] represents the latest development in relevant knowledge but the detailed description has yet to be published.

A study by Matsumoto and Kimura (1993) [4] considered a large area around Yaeyama Islands based on surveys conducted by R/V *Kaiyo* and R/V *Yokosuka*. Following a precise topographic investigation, the following factors were considered relevant to the occurrence of the Yaeyama/Meiwa earthquake:

- Submarine landslides have accumulated soil and sediment forming seabed alluvial fans.
- Seabed mud sampling indicates the alluvial fans were formed by multiple submarine landslides.
- With respect to the newest collapses and submarine landslides, the possibility of them being related to a tsunami is high because the points of seabed mud sampling were coincident with the epicenter of the Yaeyama/Meiwa earthquake.
- Submarine landslides suggest that seabed topographic points were formed in association with an earthquake because there is evidence of a devastating historical earthquake that occurred off the coast of Yaeyama Islands.



Based on the above findings from the surveys, this study considered the region of landslide occurrence to be aligned in the east–west direction, given the spread of seabed alluvial fans and the cross-sectional position corresponding to the seabed topographic points.

#### 5.4 External force from tsunami propagation analysis

To establish the external force, both earthquake motion and tsunami wave force can be considered. However, according to Dainippon Earthquake History [34], the estimated seismic intensity of Ishigaki Island is about 4, which is said to generate minimal damage through earthquake motion. Even in The Project in 2015 [33], the estimated instrumental seismic intensity of Ishigaki Island was about IV. In addition, the duration of earthquake ground motion is limited in comparison with the duration of a tsunami; therefore, the external force was set as the wave force of the tsunami. The flow rate of the horizontal component was converted to the acceleration to make it an external force of the dynamic load.

##### 1) Tsunami source model

Based on comparison of traces of the 1771 Yaeyama/Meiwa earthquake in coastal regions of Miyako and Yaeyama Islands among the source fault models used in the Tsunami Hazard Assessment Consignment Report in Okinawa Prefecture of 2012 [25], this study set Case 1 with the P1 fault as the tsunami source model ( $M_w$  8.8) because it is easily reproducible (**Fig.9 a**). As for Case 2, the closest fault (01, NI - trench - S) shown in The Project in 2015 [23] was selected as the tsunami source model. Also, with reference to the Tsunami Hazard Assessment Consignment Report in Okinawa Prefecture of 2012 [23], the slip factor (D) was adjusted such that the  $M_w$  value was 8.1 (**Fig. 9 b**).

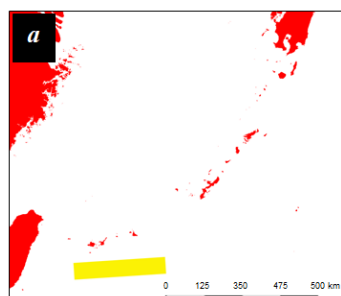
##### 2) Tsunami propagation analysis

Tsunami propagation was simulated using equations based on nonlinear longwave theory (**Table 1**). The maximum tsunami height in the insular slope point was calculated from tsunami propagation analysis. Tsunami propagation was simulated using equations based on nonlinear longwave theory, taking into account friction and advection on the seabed. This simulation used a finite difference method with a leapfrog scheme on a staggered grid. The computational time step for each grid size in the finite difference method was set according to Courant–Friedrickson–Lewy conditions to ensure stability of the calculation.

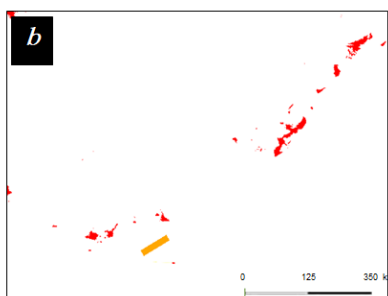
	Latitude	Longitude	Upper depth (km)	Strike (°)	Rakes (°)	Slip (°)	Length (km)	Width (km)	Slip ave. (m)	$M_w$
Case 1	23.24	125.99	2.0	265	12	90	300	70	20	8.8
Case 2	24.26	125.41	0.0	239	45	90	64	36	22	8.1

**Table 1** Details of tsunami propagation simulation

Governing equation	Non-linear long wave theory
Numerical solution	Finite-difference method (FDM) with a leapfrog scheme on a staggered grid
Calculation area	Okinawa main island and the coast of Nansei islands
Mesh resolutions	1,350 m, 450 m, 150 m, 50m
Boundary condition	Considering tsunami run up in the land area. Transmission border non reflective in the sea side.
Structures	Not consider
Calculation time	12 hours
Initial water level	Sea bed movement calculated by Okada (1992) [11]
Sea level	T.P. 0 m
Censored water depth	10-2 m
Roughness coefficient	0.025



Case 1: Tsunami source fault, Tsunami hazard assessment, Okinawa prefecture, 2011



Case 2: Tsunami source fault, Project for the Comprehensive Analysis and Evaluation of Offshore Fault Information in 2015.

**Fig. 9** Tsunami rupture models (load cases)





### 3) Waveform of water level fluctuation amount

The load condition of Case 1 was the waveform from the flow rate. The upper, middle, and lower panels of **Fig. 10 (left)** show the water level fluctuation amount (NS), flow rate (NS), and Fourier spectrum from the flow rate, respectively. As the data of water level fluctuation amount had a time step ( $\Delta t$ ) of 5 s, the Nyquist frequency was 0.1 Hz, which shows the frequency range was 0.1 Hz or less. The dominant frequency was 0.00165 Hz (10.1 min). For Case 2, the upper, middle, and lower panels of **Fig. 10 (right)** show the waveform from the water level fluctuation amount (NS), flow rate (NS), and Fourier spectrum from the water level fluctuation amount (NS), respectively. The dominant frequency of 0.000781 Hz (21 min) was longer than Case 1. In both cases, the time history of the north–south flow rate at the depth near the center of gravity of a sliding earth mass was used as a load point.

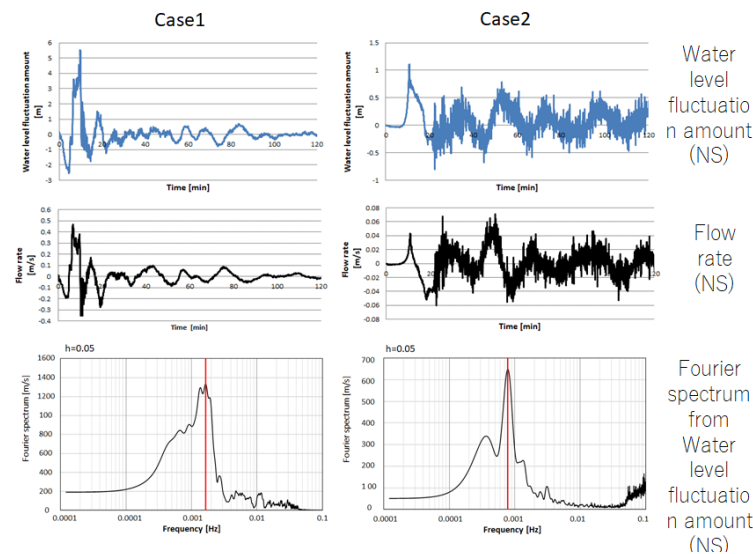


**Fig. 10** Waveforms and Fourier spectra from flow rate.

## 5.5 Seabed topographic data

### 1) Crustal structural data based

In The Project in 2015 [34], a velocity model was built for the area of the southern Nansei Islands. In creating the velocity model, we used the polymerization velocity obtained in the process of seismic profiling, together with velocity data obtained from analysis of Ocean Bottom Seismograph (OBS) seismic crustal structure surveys conducted by the Japan Coast Guard.

### 2) Soil modulus

The velocity structure model was constructed for the area of the southern Nansei Islands areas as part of the work of The Project in 2015 [23]. This study used the polymerization velocity obtained in the process of a multichannel reflection seismic data, together with OBS velocity data derived from analysis conducted by the Japan Coast Guard. Thus, the shear speed of the seabed was established as 550 m/s.

### 3) Adhesive strength test

Based on the priority study from Chen *et al.* (2006) [27] of laboratory tests, the strength of a test sample for the submarine landslide point at a depth of about 2,000 m was taken as an intermediate value of the strength of land-based mudstone (Shimajiri-mudstone:  $c = 25 \text{ kN/m}^2$ ,  $\phi = 30^\circ$ ). However, the initial value of  $\phi$  was reduced to  $20^\circ$  to ensure subsidence would occur up to a depth of 2400 m.

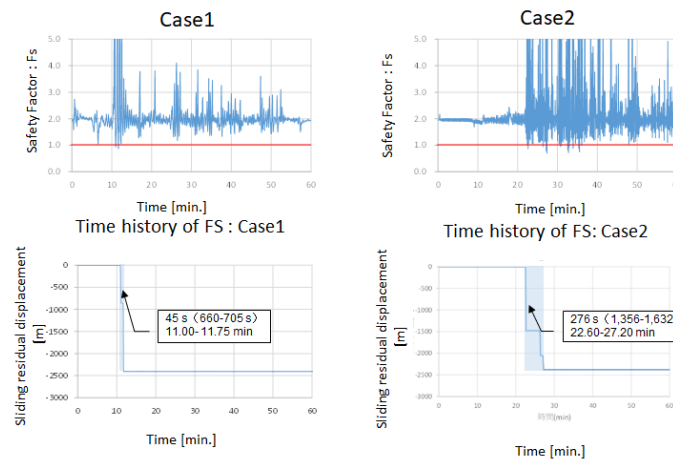


Fig. 5-10 Application of submarine landslide duration determined using the Newmark method

### 5.6 Application of submarine landslide duration using the Newmark method

Given that the duration of a submarine landslide is unknown, Hiraishi *et al.* (2001) [3] performed numerical calculations by changing the duration from 30–90 s. We applied the same process for submarine landslides in this study using the Newmark method [28] as dynamic load.

### 5.7 Calculation of duration of submarine landslides using the Newmark method

The safety factor of submarine landslides of waveforms is shown in the upper panels of Fig. 10. The sliding residual displacement of the waveforms is shown in the lower panels of The sliding residual displacement was eventually 2,400 m in both cases. The occurrence time for Case 1 was 45 s (elapsed time: 660–705 s), while that for Case 2 was 276 s (elapsed time: 1,356–1,632 s), which rounds with 280 s (Fig. 10).

### 5.8 Analysis of tsunami propagation by submarine landslides

Using the calculated external forces and slope failure durations, tsunami propagation analyses were performed for the slope failures (two cases) using seabed topographic data before and after slope failure. In this study, tsunami heights were calculated for the Yaeyama/Meiwa tsunami in A region. However, the amount of seabed topographic variation did not follow the formula of Okada (1992) [26]; instead, it was entered directly.

In Case 1, the calculated maximum tsunami height at Iwasaki, Miyarawan, and Shirahozaki was 20.86, 19.14, and 21.02 m, respectively, whereas the height of the tsunami trace at each of these locations was 30 m ( $K = 0.944$ ,  $\kappa = 1.519$ ). In Case 2, the calculated maximum tsunami height at Iwasaki, Miyarawan, and Shirahozaki was 5.01, 6.65, and 8.69 m, respectively ( $K = 2.217$ ,  $\kappa = 1.677$ ). Thus, reasonable agreement was obtained for Case 1 with short landslide duration. However, despite the conformity, Case 1 is considered to represent a magnitude less than the level of Mw 8.8 of the 1771 Yaeyama/Meiwa earthquake. Considering the submarine landslide also occurred at  $M_w$  8.1, debris at the site of the landslide extended to the east in this seabed area. In Case 2+, a doubly extended area, which involved simultaneous failure of region A and region B, was added in the eastward direction as shown in Fig. 11. In this scenario, the calculated maximum tsunami height at Inoda was 15.57 m ( $K = 1.418$ ,  $\kappa = 1.655$ ).

The occurrence time of sliding residual substantial for Case 2 was 198 s (elapsed time: 1,380–1,578 s). Here, the calculation of duration of submarine landslides was made Case 2 ++ using sliding residual substantial for Case 2 was 198 s (elapsed time: 1,380–1,578 s), which rounds with 200 s, using a doubly extended area of Case 2+. In this scenario, the calculated maximum tsunami height at Inoda was 20.13 m ( $K = 1.131$ ,  $\kappa = 1.559$ ).

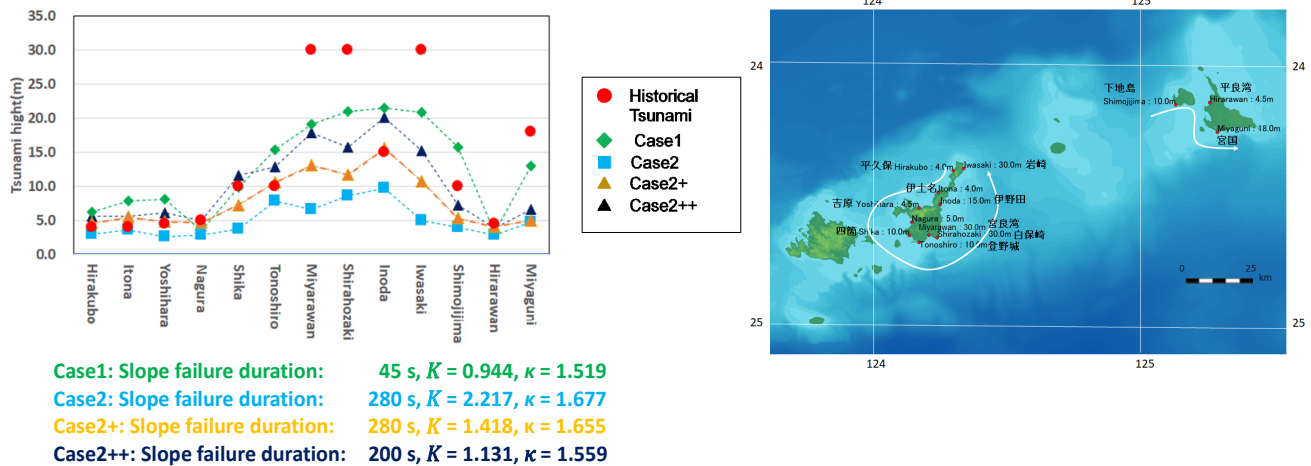


Fig.11 Comparison of historical tsunami traces and maximum calculated tsunami heights

## 5.9 Findings

The amount of seabed topographic variation did not follow the formula of Okada (1992) [26]; instead, it was entered directly and comparison was undertaken between the historical tsunami traces and the maximum coastal tsunami heights of each case. Thus, the tendency of the 1771 Yaeyama/Meiwa earthquake tsunami was reproduced. In addition, using the difference of landslide duration, this study performed analyses of tsunami propagation caused by landslides and this study found that the influence of duration has considerable effect on maximum coastal tsunami height.

A region and B region where the spread of where seabed alluvial fans had formed assumed landslides occur at the same time. For the submarine landslides caused by the tsunami associated with an event of  $M_w$  8.1, based on seismic reflection data and the fault, the execution of tsunami propagation analyses produced coastal tsunami heights of  $\sim 20$  m. At Inoda point on the eastern coast of Ishigaki Island, result was obtained good reproducibility of 15 m of historical tsunami trace and  $\sim 15$  m of maximum tsunami height calculated in Case 2 +. Here, the calculation of duration of submarine landslides was made Case 2 ++ using sliding residual substantial for Case 2 was 200 s, the calculated maximum tsunami height at Inoda was 20.13 m ( $K = 1.131$ ,  $\kappa = 1.559$ ).

## 6. References

- [1] Imamura, F., Yoshida, K., Andrew, M. (2001), The 1771 Meiwa earthquake in Ishigaki Island in Okinawa Prefecture Numerical Method of Tsunami Stone Movement, *Proceeding of Coastal Engineering*, Coastal Engineering Committee, JSCE, Vol. 48, pp.346-350. [in Japanese]
- [2] Okamura, Y., Nishizawa, A., Fujii, Y. (2018), Source of the 1771 Yaeyama tsunami, *Japan Geoscience Union Meeting 2018*, HDS10-03. [in Japanese]
- [3] Hiraishi, T, Shibaki, H., and Hara, N. (2001), Numerical Simulation of Meiwa-Yaeyama Earthquake Tsunami in Landslide Model with Circular Rupture, *Proceeding of Coastal Engineering*, Vol.48, pp.351-355. [in Japanese]
- [4] Matsumoto, T. and Kimura, M. (1993), Detailed Bathymetric Survey in the Sea Region of the Estimated Source Area of the 1771 Yaeyama Earthquake Tsunami and Consideration of the Mechanism of Its Occurrence, Vo. 45, *Second volume of "JISHIN"*, pp.417-426. [in Japanese with English abstract]
- [5] Tsuji, K., Ueda, K. (1996) : Tsunami in Kagoshima Gulf with the Anei Sakurajima eruption, *Proceeding of Volcanological Soc. of Japan*, 186. [in Japanese]
- [6] Normanbhoy N. and K. Satake (1995), Generation mechanism of tsunamis from the 1883 Krakatau eruption. *Geophys. Res. Lett.*, 22, 4, pp.509-512. [7] Lander, J. F. and P. A. Lockridge (1989), United States Tsunamis 1690-1988, Pub. 41-2, *National Geophysical Data Center*, 265 pp.



- [7] Lander, J. F. and Lockridge, P. A. (1989), Uses of a tsunami data base for research and operations (abstract), *EOS Trans., Amer. Geophys. Union* 67, 1003.
- [8] Yoshimoto, M., Takarada, S., Takahashi, R. (2007), Eruptive history of Hokkaido-Komagatake volcano, northern Japan, *The Journal of the Geological Society of Japan*, 113, new and revised edition, pp.81-92.
- [9] Satake (2007), Volcanic origin of the 1741 Oshima-Oshima tsunami in the Japan Sea. *Earth Planets Space*, 59, pp.381-390.
- [10] Tsuji, Y., Hino, T. (1993), Damage and Inundation Height of the 1792 Shimabara Landslide Tsunami along the Coast of Kumamoto Prefecture, *Bulletin of the Earthquake Research Institute*, University of Tokyo, Vol. 68, No. 2, pp.91-176. Toshiji and Hino, 1993
- [11] Baba, T., H. Matsumoto, K. Kashiwase, T. Hyakudome, Y. Kaneda, and M. Sano (2012). Micro-bathymetric evidence for the effect of submarine mass movement on tsunami generation during the 2009 Suruga Bay earthquake, Japan., in (ed) Yamada *et al.*, *Submarine Mass Movements and Their Consequences. Advances in Natural and Technological Hazards Research*. 31, 485-495, Springer.
- [12] Friz H. M., F. Mohammed and J. Yoo (2009). Lituya Bay Landslide Impact Generated Mega-Tsunami 50th Anniversary. *Pure appl. geophys.* 166, 153-175. doi:10.1007/s00024-008-0435-4
- [13] Weiss R., H. M. Fritz, and K. Wunnemann (2009). Hybrid modeling of the mega-tsunami in Lituya Bay after half a century. *Geophys. Res. Lett.*, 36, L09602; doi:10.1029/2009GL037814.
- [14] Chicxulub - Earth Impact Database (2011) <http://www.passc.net/EarthImpactDatabase/chicxulub.html> (2019.03.14, access)
- [15] Ohyagi, N. (2004), Landslides at the bottom of the sea and lake, Geographical geology recognition and terminology, Geological Geology Terminology Committee, Japan landslide society, II. Chapter 9, pp.187-2014, ISBN4902628007. [in Japanese]
- [16] Heezen, B. C. and Ewing, M. (1952), Turbidity currents and submarine slump, and 1929 Grand Banks earthquake, *Am. Jour. Science*, Vol. 250, pp. 849 -873.
- [17] Gibo, S., Nakamura, M., Higa, Y., Yoshizawa, M. (2003), The Shear Strength of Strongly Weathered and Fractured Mustones for Slope Stabability Analysis – Stability of slopes in the mudstone area of the Shinmajiiri-group, Okinawa -, *Trans. of J S I D R E*, No.227, pp.113-118. [in Japanese with English abstract]
- [18] Hatori, T. (1988), Tsunami Magnitudes and Source Areas along the Ryukyu Islands, *ZISIN2*, Vol. 41, pp.541-547. [in Japanese with English abstract]
- [19] Kato, Y. (1987), Run-up Height of Yaeyama Seismic Tsunami (1771), *ZISIN2*, Vol. 40, pp.377-381. [in Japanese with English abstract]
- [20] Kawana, T. and Nakada, T. (1994), Timing of Late Holocene Tsunamis Originated around the Southern Ryukyu Islands, Japan, Deduced from Coralline Tsunami Deposits, *Journal of Geography*, Vol.103, No.4, pp.352-376. [in Japanese with English abstract]
- [21] Kawana, K., and Imamura, F. (2010), Historical and geological evidence of boulders deposited by tsunamis, southern Ryukyu Islands, Japan, *Earth-Science Reviews* 102 (1-2), pp.77-99.
- [22] Kyuyou, Okinawa culture historical materials collection 5, Kadokawa Sophia Bunko, 793p., 2011. [in Japanese]
- [23] Project for the Comprehensive Analysis and Evaluation of Offshore Fault Informatics (2015), Headquarters of Earthquake Res. Promotion, Ministry of Education, Culture, Sports, Science and Technology. [in Japanese]
- [24] Dainippon Earthquake History (1943), new and revised edition. Vol. 2, pp.1621 - 1783, Association of earthquake disaster prevention (Shinsaiyouboukyoukai). [in Japanese]
- [25] Tsunami Hazard Assessment Consignment Report in Okinawa Prefecture of 2012, Okinawa Prefecture. [in Japanese]
- [26] Okada, Y. (1992), Internal deformation due to shear and tensile in a half-space, *Bull. Seismol. Soc. Am.*, Vol. 85, pp. 1018-1040.
- [27] Chen, C., Gibo, S., Sasaki, K., Nakamura, S. (2007), Classification of landslide types observed in the area of Shimajiri-madstone., Okinawa Island - For the risk evaluation of Landslide -, *Landslides*, Vol.43, No.6, pp.339-350. [in Japanese with English abstract]
- [28] Newmark, N.M. (1965), Effects of Earthquake on Dams and Embankments, *Geotechnique*, Vol.15, No.2, pp.137-160.
- [29] Horii, K., Tateyama, K, Uchida, Y., Koseki, J., Tatsuoka, F. (1997), Seismic failure deformation prediction of railway embankment by Newmark method, *32th Geotechnical research presentation*, pp.1895-1896. [in Japanese]